ECOLOGY LETTERS

Ecology Letters, (2016) doi: 10.1111/ele.12605

LETTER

On the context-dependent scaling of consumer feeding rates

Daniel Barrios-O'Neill,[1]* Ruth Kelly,[1] Jaimie T. A. Dick,[1] Anthony Ricciardi,[2] Hugh J. MacIsaac[3] and Mark C. Emmerson[1]

Abstract

The stability of consumer–resource systems can depend on the form of feeding interactions (i.e. functional responses). Size-based models predict interactions – and thus stability – based on consumer–resource size ratios. However, little is known about how interaction contexts (e.g. simple or complex habitats) might alter scaling relationships. Addressing this, we experimentally measured interactions between a large size range of aquatic predators (4–6400 mg over 1347 feeding trials) and an invasive prey that transitions among habitats: from the water column (3D interactions) to simple and complex benthic substrates (2D interactions). Simple and complex substrates mediated successive reductions in capture rates – particularly around the unimodal optimum – and promoted prey population stability in model simulations. Many real consumer–resource systems transition between 2D and 3D interactions, and along complexity gradients. Thus, Context-Dependent Scaling (CDS) of feeding interactions could represent an unrecognised aspect of food webs, and quantifying the extent of CDS might enhance predictive ecology.

Keywords

Body size, density dependence, functional response, habitat complexity, invasive species, population stability, predator–prey dynamics, scaling, Type II, Type III.

Ecology Letters (2016)

INTRODUCTION

In ecology, complexity and contingency are pervasive, and so the notion that many patterns and processes can be unified by considering organisms as consumers and processors of energy – embodied within the metabolic theory of ecology (MTE; Brown *et al.* 2004) – is appealingly parsimonious. Because MTE offers a mechanistic link between temperature, body size and metabolic rate, it follows that the feeding rates of consumers (i.e. their energy acquisition) should reflect intrinsic metabolic demand. However, generalising consumer feeding rates to metabolic first principles remains problematic, particularly for two reasons: (1) because feeding rates emerge from the relative performance of at least two agents – the consumer and the resource (Ohlund *et al.* 2014); and (2) because historical energy acquisition and storage can dictate the necessity for feeding interactions when consumers encounter resources (Maino *et al.* 2014).

In its most basic form, the interaction between consumer and resource can be formalised as the functional response (Holling 1959; Real 1977), defining the relationship between resource acquisition by a single consumer and resource density:

$$N_e = bN \tag{1a}$$

$$N_e = \frac{bN^{q+1}}{1 + bhN^{q+1}} \tag{1b}$$

where N_e is the *per capita* rate of resource consumption (individuals s^{-1}), b is the capture rate or search coefficient of the consumer ($m^2\ s^{-1}$ or $m^3\ s^{-1}$) – for simplicity, we treat capture rates and search coefficients as synonymous (but see Kalinkat *et al.* 2013) – N is the resource density (individuals m^2 or m^3, constant in time), h (s) is consumer handling time, strictly incorporating the processes of subjugation and ingestion (but often reflecting digestion: see supplementary materials) and q is the scaling exponent, defining the extent to which the functional response departs from a decelerating hyperbola (Type II) towards a sigmoidal (Type III) form. Where $q = 0$ capture rates are independent of N. Where $q > 0$ capture rates depend explicitly on N, often reflecting consumer learning, whereby capture rates increase with N, resulting from: (1) increased encounters (e.g. switching from passive to active searching), or (2) an increased ratio of captures to encounters.

Across the biosphere, capture rates scale positively with consumer mass (Fig. 1), but there are layers of complexity nested within this trend (Pawar *et al.* 2012; Rall *et al.* 2012). For example, consumers often exhibit lower capture rates towards relatively large or small resources (Osenberg & Mittelbach 1989; Persson *et al.* 1998; Aljetlawi *et al.* 2004; Vonesh & Bolker 2005). As a result, at the local scale, capture rates often distribute unimodally along a spectrum of consumer (M_C), resource (M_R), body mass ratios ($\frac{M_C}{M_R}$), delineating a series of 'sub webs' nested within the general trend (Fig. 1, blue and orange: Woodward *et al.* 2005; Rall *et al.* 2012). Isolating the dependence of capture rates on $\frac{M_C}{M_R}$ yields a general scaling for capture rates with consumer mass (Pawar *et al.* 2012):

[1]*Institute for Global Food Security, School of Biological Sciences, Queen's University Belfast, 97 Lisburn Road, Belfast, BT9 7BL, Northern Ireland*
[2]*Redpath Museum, McGill University, 859 Sherbrooke Street West, Montreal, QC, H3AOC4, Canada*
[3]*Great Lakes Institute for Environmental Research, University of Windsor, Windsor, ON, N9B 3P4, Canada*
**Correspondence: E-mail: d.barrios-oneill@qub.ac.uk*

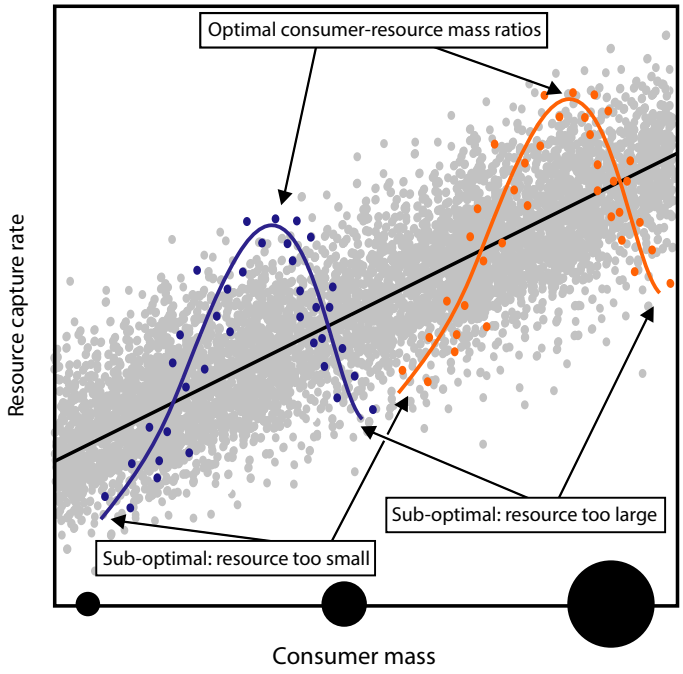

Figure 1 Conceptualised scaling of capture rates (*b*: eqn 1) with consumer mass. Larger consumers require more energy to survive, grow and reproduce, leading to a general positive association between mass and capture rates (grey points and black line). When resources are suboptimally sized (relatively small or large) capture rates decline, leading to a dependency of capture rate on consumer–resource mass ratio, and resulting in unimodal associations (orange and blue points and lines) – termed 'sub-webs' – nested within the general trend.

$$b = a_0 M_C^{\alpha} f\left(\frac{M_C}{M_R}\right) \quad (2)$$

where b is the consumer capture rate (eqn 1), a_0 is a scaling constant, α is the scaling exponent and $f(\frac{M_C}{M_R})$ is a unimodal function of M_C and M_R (Fig. 1, blue and orange).

Non-linear feeding interactions (eqn 1b, where h and/or $q > 0$) are a crucial component of the scaling of consumer feeding rates for two reasons: (1) because measuring interactions at fixed resource densities can under- or overestimate feeding rates, which are rarely linear in nature (Jeschke *et al.* 2004); and (2) because the size dependencies of non-linear feeding interactions – in terms of shape (that is, functional response Type – primarily q and b) and magnitude (primarily h) – are critical for the coexistence of consumer–resource pairs (Murdoch 1969; Kalinkat *et al.* 2013), and promote stability in tri-trophic food chains or complex food webs (Williams & Martinez 2004; Brose *et al.* 2006). In particular, small consumer–resource mass ratios can result in destabilising Type II functional responses ($q = 0$) due to high resource exploitation at low resource densities. As ratios increase, responses systematically transition ($q > 0$) towards stabilising Type III sigmoid curves typified by low resource exploitation at low resource densities (Kalinkat *et al.* 2013). Size-based approaches to defining interactions are not without limitations, but their value is manifest in linking MTE with local-scale community dynamics and in making useful predictions at these scales, for example, describing the consequences of species loss from food webs (Schneider *et al.* 2012).

We argue that understanding the community-level consequences of extinctions, invasions and the impacts of anthropogenic stressors will depend acutely on resolving local scaling within subwebs. Generalisations of consumer feeding around temperature and body mass constitute only part of the means to this end, particularly because resources (i.e. prey) utilise refuge space (Barrios-O'Neill *et al.* 2015), employ defensive adaptations (Osenberg & Mittelbach 1989) and may not consistently co-occur with consumers (Englund & Leonardsson 2008) – any of which can force suboptimal consumer feeding rates. In addition, consumer capture rates depend on how consumers and resources converge across the landscape (i.e. relative velocity) and the dimensionality and size of their respective detection regions (Pawar *et al.* 2012). Detection region size, in particular, increases substantially when consumers switch from searching over a surface (2D interactions) to searching through a volume (3D interactions). Such switches are likely pervasive in bentho-pelagic aquatic systems where consumers migrate within and between habitats (Barrios-O'Neill *et al.* 2014b). Indeed, relative velocity and detection region are also independently modified by habitat structure (Manatunge *et al.* 2000), which may or may not covary with dimensionality. At local scales, the magnitude and shape of consumer–resource interactions can therefore vary with context in space and time – primarily through the modification of capture rates. Thus, some degree of systematic variability is intrinsic to the size scaling of consumer feeding rates; yet attempts to understand and quantify this variability are lacking, resulting in a substantial knowledge gap. Moreover, addressing this gap empirically requires the simultaneous incorporation of consumer size, resource density and contexts such as dimensionality and complexity – together representing a considerable logistical challenge

Here, in the largest empirical study of its kind, we resolve the functional responses of a range of aquatic ectotherm vertebrate and invertebrate predators – covering four orders of magnitude in body mass between ~ 4 and ~ 6400 mg (Table 1) – feeding upon a successful invasive Ponto-Caspian prey species, the corophiid amphipod *Chelicorophium curvispinum* Sars 1895. In 1347 laboratory trials, we quantified the size scaling of functional response parameters across different spatial contexts reflecting the constantly shifting distribution of *C. curvispinum* in lacustrine systems: swimming in the water column – a structurally simple 3D context – and established on a range of structurally simple and complex 2D substrates. We hypothesised that: (1) 2D contexts would yield reductions in consumption concomitant with reductions in capture rates when compared to the 3D context; (2) that structural complexity would further reduce consumption by the same mechanism and (3) that, given a unimodal distribution of capture rates (Fig. 1), reductions would be largest for consumers with optimal capture rates in relation to resource size. Population dynamical simulations parameterised with context-specific functional response models further illustrate how stability regimes might shift with interaction context, whereby increasing substrate complexity eliminates extinction and reduces instability in prey populations across the entire spectrum of

Table 1 Body masses (wet weights in mg) for each predator/size treatment and predator–prey body mass ratios (*R*) with *Chelicorophium curvispinum*

Predator	Rank mass (small > large)	No. trials (all contexts)	Mean mass (mg)	SD	*R*
Gammarus d. celticus	1	63	4.38	0.55	1.12
Gammarus pulex	2	63	4.56	0.5	1.17
Gammarus d. celticus	3	63	8.13	1.81	2.08
Gammarus pulex	4	63	8.59	1.87	2.2
Hemimysis anomala	5	91	17.49	2.94	4.49
Mysis salemaai	6	34	19.15	1.56	4.91
Gammarus d. celticus	7	63	22.43	5.16	5.75
Gammarus pulex	8	63	24.03	5.35	6.16
Gammarus d. celticus	9	63	53.84	8.42	13.81
Gammarus pulex	10	63	54.78	8.6	14.05
Gammarus d. celticus	11	91	80.37	12.58	20.61
Gammarus pulex	12	91	83.88	12.69	21.51
Pungitius pungitius	13	91	156.68	36.64	40.17
Gasterosteus aculeatus	14	63	402.87	50.98	103.3
Gasterosteus aculeatus	15	63	664.73	112.71	170.44
Perca fluviatilis	16	63	1118.97	284.95	286.91
Gasterosteus aculeatus	17	69	1225.64	217.53	314.27
Salmo trutta	18	69	1865.42	217.65	478.31
Barbatula barbatula	19	63	2694.05	505.52	690.78
Salmo trutta	20	54	6433.96	1568.49	1649.73

predator body sizes. We then go on to develop a framework outlining the Context-Dependent Scaling (CDS) of consumer feeding rates.

MATERIAL AND METHODS

Animal collection and maintenance

We used five species of predatory fish and four predatory crustaceans – and several size classes of some of these predators – resulting in twenty discrete predator–prey body mass ratio pairings, with overlapping body mass distributions covering body mass ratios of ~ 1 to ~ 1600 (Table 1). *Chelicorophium curvispinum* was used as prey in all trials and was collected from Lough Derg, Co. Tipperary (52.92583° N, 8.27913° W). Nine-spined stickleback *Pungitius pungitius* (Linnaeus 1758) and the mysid shrimps *Mysis salemaai* Audzijonyte and Väinölä, (2005) and *Hemimysis anomala* (Sars 1907) were collected from the same location. The gammarid amphipods *Gammarus pulex* (Linnaeus 1758) and *Gammarus duebeni celticus* Stock and Pinkster 1970 were collected from a tributary of the River Lagan, Co. Antrim (54.50914° N, 5.97018° W) and the Gransha River, Co. Down (54.5484° N 5.81950° W), respectively. Stone loach *Barbatula barbatula* (Linnaeus 1758) were also collected from the Lagan tributary. Three-spined stickleback *Gasterosteus aculeatus* (Linnaeus 1758) were collected from Oxford Island Nature Reserve (54.49617° N, 6.38173° W), whereas brown trout *Salmo trutta* (Linnaeus 1758) and perch *Perca fluviatilis* (Linnaeus 1758) were obtained from the Ballinderry River Enhancement Association and Clune Fishery respectively. Each predator species and/or size category thereof was maintained separately in continuously aerated 25 μm filtered source water at 12° C on a 12 L : 12 D photoperiod. All predators were fed *ad libitum* with *C. curvispinum* for at least 10 days, and starved in isolation for 24 h prior to trials. *C. curvispinum* stock was maintained under an identical temperature and lighting regime in 40 L aquaria with continuously aerated unfiltered water from the Lagan tributary, which was changed every 2–3 days. Although *C. curvispinum* can survive for long periods of time under laboratory conditions (Barrios-O'Neill, personal observation), we ensured negligible background mortality during feeding trials by collecting new batches of *C. curvispinum* from the field at 10 day intervals.

Experimental trials

Chelicorophium curvispinum is found swimming in the water column and also established in mud tubes among the benthos (Van den Brink *et al.* 1993; Noordhuis *et al.* 2009). It can achieve very high abundances on spatially complex substrates such as biogenic mussel reefs, and will also establish on simple substrates, particularly on muddy sediments and on anthropogenic structures (Barrios-O'Neill, personal observation; van Riel *et al.* 2006). Therefore, we aimed to derive the functional responses of the resident predators across three spatial contexts reflecting the distribution and behaviour of *C. curvispinum*: swimming in the water column (a 3D context), established in mud tubes on simple substrates and established in mud tubes on complex substrates (2D contexts). Here, although complexity effects in 2D contexts can be isolated, changes in prey behaviour and arena edge effects prevent the explicit isolation of dimensionality.

Prey *C. curvispinum* were initially coarsely sorted for size, yielding experimental individuals with a mean wet weight of 3.9 mg ± 0.05 SE. All trials were conducted in circular arenas of 11.5 cm Ø filled with 700 mL of filtered (25 μm) Lough Derg source water. Arena treatments were designed to reflect three aforementioned contexts: 'swimming' containing only water, 'simple' containing ~ 20 g of 250–500 μm diameter (Ø) sediment particulates or 'complex' containing 20 g sediment particulates and 20 artificial black pebbles (18.6 mm Ø,

6.1 mm tall). Prey were introduced into arenas over a minimum density range of 2, 4, 6, 10, 25, 40 and 100 individuals and with replication of $n \geq 3$. In instances where predator feeding did not become prey saturated, the density range was increased, particularly for some larger predators with higher feeding rates, where densities of up to 300 prey were used. Maximum prey density in experimental trials translates to a maximum field abundance of ~ 29 000 individuals per m^2, which is commonly observed in the Rhine River and its tributaries, although during invasion peaks maximum actual field abundance can be an order of magnitude greater (Van den Brink *et al*. 1993).

To allow *C. curvispinum* in spatially simple and complex 2D treatments time to construct tubes from sediment particulates, a period of 4 h elapsed before the introduction of single starved predators into all treatments. Trials ran for 24 h and were terminated on the removal of predators, after which surviving prey were counted. Refer to supplementary materials for further details on setup and behavioural observations. Here, we retain data from all experimental trials regardless of whether consumption occurred for three reasons: (1) because predation was naturally infrequent with the smallest consumers; (2) because non-consumption at low prey densities can result in Type III functional responses and (3) because disregarding natural variation (e.g. Toscano & Griffen 2014) in consumption is tantamount to subsampling.

Predator-free controls ($n \geq 3$) across all densities and treatments indicated that background prey mortality was negligible and did not affect our results.

Functional response model

Eqn 1b assumes that prey density remains constant in time – an assumption that is violated over the course of an experimental trial unless consumed prey are immediately replaced. Therefore, we adopt a generalised functional response model that accounts for the non-replacement of prey as they are consumed (Real 1977; Vucic-Pestic *et al*. 2010):

$$N_e = N_0(1 - exp(bN_0^q(hN_e - T))) \quad (3)$$

where N_e is the number of prey eaten, N_0 is the initial prey density, b is the search coefficient or capture rate (arena volume/footprint day^{-1}) which, in combination with the scaling exponent, q, gives the density-dependent capture rate (bN_0^q), h is the handling time (day^{-1}) and T is the total time. Note that units reflect experimental scale and time. We used maximum likelihood (Bolker 2010) to estimate modal parameters for each predator–treatment combination and prevented negative estimates of q (Vucic-Pestic *et al*. 2010): for Type II functional responses, where $q = 0$ eqn 3 collapses to the random predator equation (Rogers 1972).

Scaling relationships

Following the quantification of individual predator–prey functional responses, we tested for systematic relationships across three experimental contexts between predator–prey body mass ratios and the capture rates, handling times and scaling exponents derived from eqn 3. We treat predator–prey body mass ratios as the focal explanatory variable to appropriately scale relationships with consumer feeding parameters; where predators are close in size to their prey, small changes in predator mass result in large changes to predator–prey mass ratios. Being constrained by a single-prey species study system, we are unable to explicitly isolate the effects of predator–prey mass ratios from predator mass as in eqn 2 and, therefore, cannot address general scaling beyond the subweb level.

Based on the search space model of Pawar *et al*. (2012), we hypothesised that context-driven differences in consumption would manifest through changes in consumer capture rates (Introduction: hypothesis (1) and hypothesis (2)). For rigour, however, we initially explored global data sets (of b, h and q respectively: eqn. 3) by comparing polynomial models including experimental context as an explanatory variable against models retaining only body mass ratio as explanatory. Throughout model selection and fitting, we opt to transform dependent and independent variables by $log_{10}(x + 1)$ to avoid problems at 0. ANOVAs between models provided initial justification for splitting capture rates by context ($F_{2,55} = 12.01$, $P < 0.001$) and amalgamating handling times ($F_{2,45} = 0.10$, $P = 0.906$) and scaling exponents ($F_{2,45} = 0.70$, $P = 0.501$). We further hypothesised that reductions in capture rates would be most pronounced for those consumers with the highest rates (Introduction: hypothesis (3)). Therefore, we tested capture rate scaling for deviations from linearity via removal of quadratic terms for each context: 'swimming' ($F_{1,17} = 42.10$, $P < 0.001$); 'simple' ($F_{1,17} = 0.70$, $P = 0.077$) and 'complex' ($F_{1,17} = 0.12$, $P = 0.730$). The contexts 'swimming' and 'simple' exhibited non-linear unimodal distributions, therefore we used generalised Ricker functions to describe these data (Persson *et al*. 1998):

$$log_{10}(b + 1) = \beta\left(\frac{log_{10}(R + 1)}{\gamma} exp\left(1 - \frac{log_{10}(R + 1)}{\gamma}\right)\right)^{\propto} \quad (4)$$

where b is the capture rate, R is the predator–prey body mass ratio and β, γ and α are constants. We fitted eqn 4 using a non-linear least-squares regression approach. In contrast, the context 'complex' exhibited a power law relationship. Therefore, we fitted a linear model to log_{10} transformed data using a least-squares approach and did not extrapolate below the body mass ratio at which predation did not occur ($b = 0$).

Global cross-context consumer handling times were described by an exponentially declining function – primarily as a simple means to capture observed data – but also reflecting the mechanistic impossibility of negative handling times, and previously observed exponential declines with consumer mass or consumer–resource mass ratios (Aljetlawi *et al*. 2004; Kalinkat *et al*. 2013). We fitted the following using non-linear least-squares regression:

$$log_{10}(h + 1) = \delta\, exp(\varepsilon log_{10}(R + 1)) \quad (5)$$

where h is the handling time, R is the predator–prey body mass ratio and δ and ε are constants.

For scaling exponents, we retain the cross-context polynomial function, describing a u-shaped relationship with

predator–prey body mass ratios (refer to the legend of Fig. 2 for details).

Population dynamics

Context-specific functional response models (i.e. context-specific capture rates combined with cross-context handling time and scaling exponent models) were used to modify the Rosenzweig-MacArthur model of predator–prey dynamics (Rosenzweig & Macarthur 1963):

$$\frac{dN}{dt} = rN\left(1 - \frac{N}{K}\right) - \left(\frac{bN^{q+1}}{1 + bhN^{q+1}}\right)P \quad (6a)$$

$$\frac{dP}{dt} = \left(\frac{bN^{q+1}}{1 + bhN^{q+1}}\right)eP - mP \quad (6b)$$

where P and N are predator and prey population sizes (number of individuals), respectively, t is time, r is the growth rate of the prey, K is the prey carrying capacity, e is predator assimilation efficiency and m is predator mortality. Functional response parameters are modified by body mass ratios according to global handling time and scaling exponent models, h and q, whereas capture rate models, b, are specific to contexts 'swimming', 'simple' and 'complex'. Here ,we focus on the local minima and maxima of prey population size, and resulting population instability (coefficient of variation) in the context of the invasion success of *C. curvispinum*.

RESULTS

Scaling relationships

Predator capture rates exhibited unimodal relationships (eqn 4) with predator–prey body mass ratios for swimming prey in 3D environments (Fig. 2a: all model parameters significant at $P < 0.05$; refer to figure legend) and prey established on simple 2D substrates (Fig. 2b: all model parameters significant at $P < 0.05$; refer to figure legend). On simple 2D substrates predation by the smallest size classes of predators was suppressed ($b = 0$), whereas the optimum capture rate was lowered and upshifted along the body mass ratio axis, supporting hypothesis (1) (Fig. 2b as compared with Fig. 2a). In contrast, the presence of habitat structure – i.e. prey established on complex 2D substrate – resulted in a marked flattening of the relationship between capture rates and predator–prey body mass ratios into a shallow power law relationship (Fig. 2c as compared with Fig. 2b, linear coefficient = 0.05 ± 0.01, $P < 0.001$), supporting

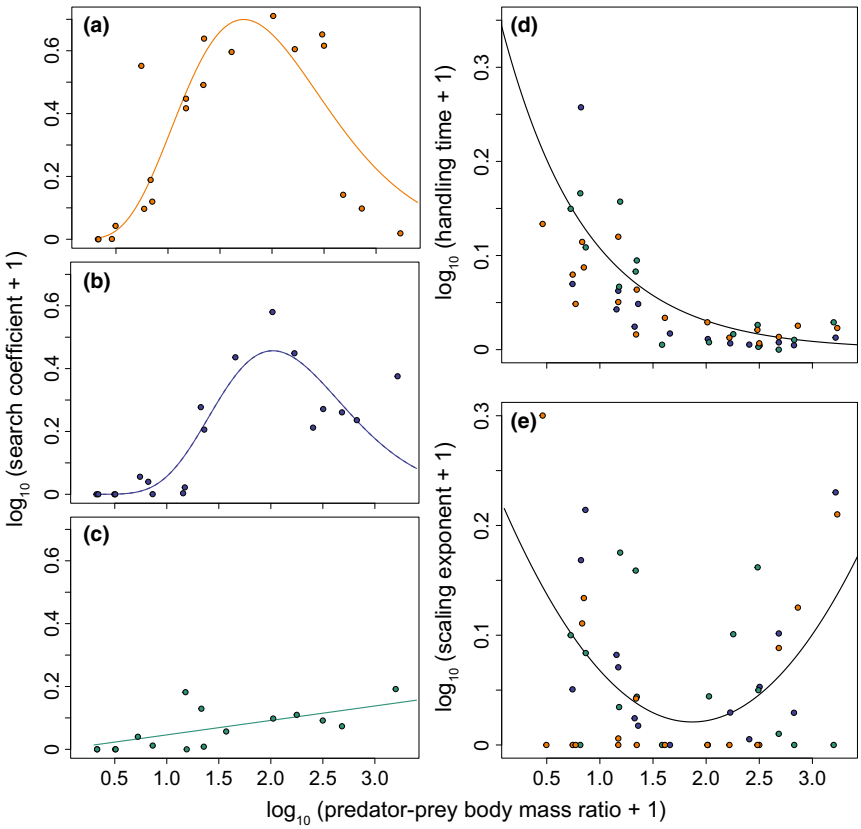

Figure 2 Scaling of functional response parameters with predator–prey mass ratios. Capture rates follow unimodal relationships for swimming prey (a: orange) and prey on simple substrates (b: blue), but follow a power law for prey on complex substrates (c: green): (a) $\beta = 0.70 \pm 0.08$ (estimate ± SE) $P < 0.001$, $\gamma = 1.73 \pm 0.08$, $P < 0.001$, and $\alpha = 6.13 \pm 1.63$, $P = 0.002$; (b) $\beta = 0.46 \pm 0.06$, $P < 0.001$, $\gamma = 2.02 \pm 0.08$, $P < 0.001$, and $\alpha = 10.52 \pm 3.04$, $P = 0.003$; (c) coefficient = 0.05 ± 0.01, $P < 0.001$. (d) Handling times follow a global negative exponential relationship; $\delta = 0.38 \pm 0.14$, $P = 0.012$ and $\varepsilon = -1.25 \pm 0.40$, $P = 0.003$. (e) Scaling exponents are described by a global polynomial; quadratic term = 0.6 ± 0.02, $P = 0.001$, linear term = −0.23 ± 0.07, $P = 0.001$.

hypothesis (2) and hypothesis (3). Despite pronounced differences at low and intermediate body mass ratios, capture rates tended to converge at the highest mass ratios among all contexts (Fig. 2a–c).

Consumer handling times declined exponentially with increasing predator-prey body mass ratios, and relationships were qualitatively similar among contexts (Fig. 2d: orange, blue and green points). The global exponential model (eqn 5) described this trend appropriately ($\delta = 0.38 \pm 0.14$, $P = 0.012$ and $\varepsilon = -1.25 \pm 0.40$, $P = 0.003$), but tended to overestimate handling times (Fig. 2d: model line and data points).

Scaling exponents were notably variable (Fig. 2e: orange, blue and green points), with absolute Type II functional responses ($q = 0$) occurring across the range of body mass ratios, and among all predatory contexts. Despite this inherent variability, the tendency for higher scaling exponents – for increasingly Type III functional responses – to correlate with small and large predator–prey body mass ratios was evidenced by the u-shaped cross-context polynomial model (Fig. 2e: model line, all model parameters significant at $P < 0.05$; refer to figure legend).

Model parameters b, h and q (eqn 3) combine to yield context-specific functional response models (Fig. 3a–c), which demonstrate that interactions on substrates – both simple and complex – are suppressed at small predator–prey body mass ratios (Fig. 3d, $R = 1$). Generalising handling times across contexts results in identical maximum feeding rates ($1/hT$) and, therefore, leads to a convergence of predicted consumption at high prey densities (Fig. 3d, $R = 10$). However, context-specific capture rates models ensure that predicted consumption at critical low prey densities was markedly different among contexts, except at the highest mass ratios (Fig. 3d: all panels)

Population dynamics

For prey populations swimming in 3D (Fig. 4a) stability and coexistence occurred only at high and low predator–prey body mass ratios, with prey maintaining higher stable equilibria when interacting with small predators (low ratios) as compared to large predators (high ratios). As ratios increase, the stable equilibria associated with low ratios abruptly bifurcate to chaotic dynamics and/or complete population crashes, only coalescing to stability and coexistence again above body mass ratios of 1000. For prey established on simple 2D substrates (Fig. 4b), population dynamics were superficially similar to those of prey in 3D (Fig. 4a). However, the coefficient of variation (CV) – reflecting population instability – reveals that prey populations established on simple 2D substrate exhibit increased stability (i.e. a lower CV) when compared to 3D, notably at intermediate body mass rations (Fig. 4d: orange trace vs. Fig. 4d: blue trace). For prey on complex 2D substrates (Fig. 4c), coexistence ($N > 0$) occurred across the entire spectrum of predator–prey body mass ratios and, whereas populations destabilised to some degree at intermediate body mass ratios, they remained consistently stable across a greater range of body mass ratios than comparative contexts (Fig. 4d: green trace as compared with orange and blue traces). Supplementary materials detail how sensitive these differences are to K (eqn 6a) and q (eqn 4).

DISCUSSION

Our findings suggest that the scaling of consumer feeding rates can be context dependent – potentially at small spatiotemporal scales – and are largely congruent with hypotheses (1–3), supporting the contention that capture rates mediate this variation. Thus, interactions can vary within the confines of metabolic limits, simultaneously with key extraneous drivers *and* consumer body mass. Consequently, we propose a conceptual progression that moves away from framing feeding rates primarily around temperature and body size at the local scale, while still recognising that these remain fundamental predictors. We envisage a Context-Dependent Scaling (CDS) of feeding rates as consumer–resource systems move between contexts that systematically modify a consumer's search space and encounter rate with resources.

Beyond metabolic scaling

Evidence suggests that the form and magnitude of a consumer's functional response is size and temperature dependent (Englund *et al.* 2011; Rall *et al.* 2012). In turn, these dependencies dictate consumer–resource coexistence and population stability (Vucic-Pestic *et al.* 2011; Kalinkat *et al.* 2013). Functional responses also change systematically with, among other things, habitat structural complexity (Barrios-O'Neill *et al.* 2015) and dimensionality of search space (Pawar *et al.* 2012). Drivers such as these may operate equally across a range of consumer body sizes, and vary predictably in space and time (e.g. light), or instead act disproportionately on specific consumer sizes and/or vary in myriad ways in space and time (e.g. structural complexity).

Stability and coexistence between consumers and resources depends on more than temperature and body mass, as feeding rates are also demonstrably coupled to extraneous drivers including – but not limited to – dimensionality and structural complexity. For this reason, our reductive comparisons of prey population stability regimes between experimental contexts are primarily illustrative. Even if interactions within the wider community are not considered, simple consumer–resource population stability will result from the contributions of each context to modifying interactions and resultant population dynamics. Indeed, intra- and interspecific interference are particularly critical modulators in this respect because interference may scale with dimensionality and consumer size (Barrios-O'Neill *et al.* 2014a; DeLong 2014) and because higher predator cues are likely to universally modify feeding rates (Paterson *et al.* 2013). Nevertheless, these results do imply that some degree of structural complexity can be a critical determinant of coexistence and stability.

Our results suggest that intermediate predator–prey body mass ratios are aligned with both high capture rates and low scaling exponents, translating to a large – potentially destabilising – consumptive impacts where prey populations are small. The reductions in capture rates at intermediate ratios associated with complex habitat structure (Fig. 2c) – and concomitant coexistence in simulations (Fig. 4c) – suggest that structural complexity modulates destabilising interactions. In addition to this context dependency, the natural

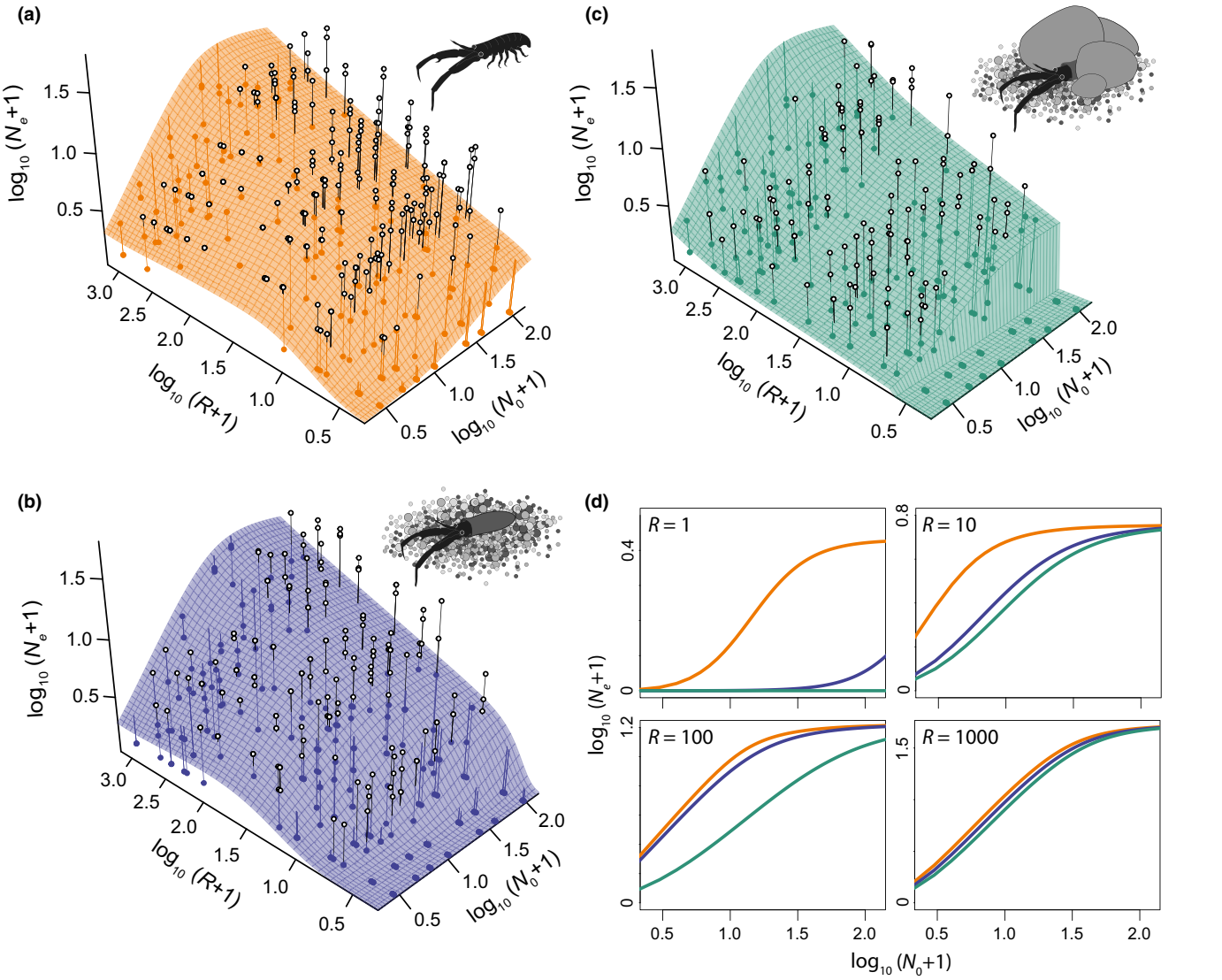

Figure 3 Functional response surfaces as defined by context-specific (Fig. 2a–c) and global parameters (Fig. 2d–e) for; (a) swimming prey; (b) prey on simple substrate and (c) prey on complex substrate. N_e is prey consumption rate, N_0 is initial prey density and R is the predator–prey body mass ratio. Points are log-transformed consumption data (open points are above model surface, filled points are below). Lines are residual distances from actual consumption rate data to predicted consumption rates defined by model surfaces. (d) Highlights differences between surfaces (a–c) across four orders of magnitude in R: 1 (0.30 log transformed), 10 (1.04 log transformed), 100 (2.00 log transformed) and 1000 (3.00 log transformed).

invertebrate–vertebrate transition with increasing consumer mass highlights the importance of species identity in determining the scaling of capture rates (Rall *et al*. 2011), particularly because species assemblages can vary in space and time (Hutchinson 1961).

Dimensionality and complexity of consumer search space

Pawar *et al*. (2012) suggest that feeding rates scale superlinearly in 3D and sublinearly in 2D, and that differences in scaling are driven by the size of consumer and resource detection regions. Although the size of our largest consumer's (*Salmo trutta*) detection region likely exceeds the size of the arena in our 3D habitat, this does not necessarily preclude detection region as the mechanism underpinning the relative differences in capture rates among our treatments due to the effects of prey crypsis and obstructed line of sight on consumer detection region in 2D habitats.

We find that interactions are broadly strongest towards swimming prey and, here, they are also acutely size structured, with larger variations in capture rates over the same range of body mass ratios. On spatially complex substrates the opposite is true, where capture rates are generally lower for a given consumer body mass, and vary less with body mass ratios. Together, these observations suggest that interactions might systematically vary beyond the 2D/3D binary. In 3D pelagic systems, feeding rates are often strongly size structured (Wahlström *et al*. 2000) and characterised by large aggregations of predators and prey. The latter is a characteristic shared by 2D carnivore-ungulate systems in open, structurally

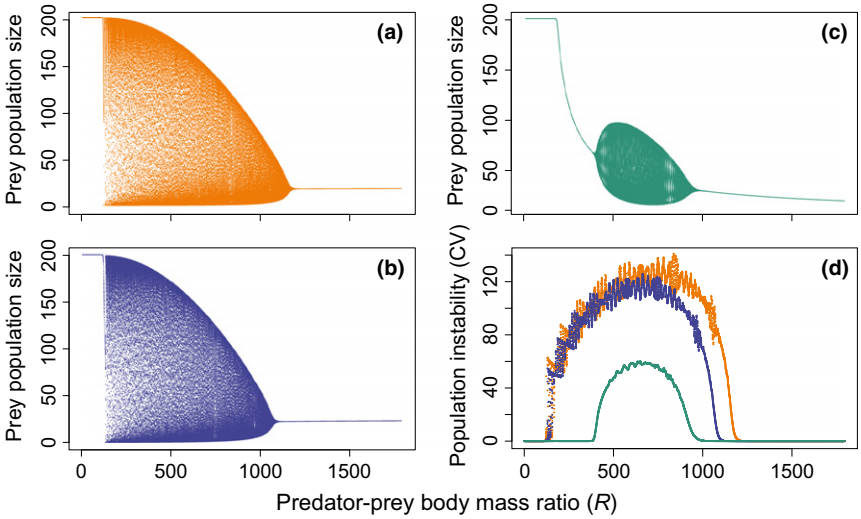

Figure 4 Prey population dynamics: prey populations sizes (N) at each of the final 30 timesteps (30 days of 10 000 day simulation runs) for a given predator–prey body mass ratio (R). Population sizes are derived from population models (eqns 6a and 6b) parametrised with context-specific functional response models (Fig. 3a–c) for: (a) swimming prey (orange trace); (b) prey on simple substrate (blue trace) and (c) prey on complex substrate (green trace). (d) Prevalence of prey population instability (CV) associated with each context (a–c).

simple grasslands (Fryxell 1995). Thus, interaction strengths may also vary continuously along gradients of environmental heterogeneity and structural complexity. Many studied 3D systems are less structurally complex than 2D systems, suggesting that the observed correlations of Pawar *et al.* might also be underpinned by complexity. However, although our experimental treatments reflect the real-world transitions of *C. curvispinum*, the link to dimensionality remains weak because refuge availability is restricted to our 2D treatment. Altogether, a deeper understanding of the relative contributions of complexity and dimensionality represents an important next step towards making tractable generalisations of consumer feeding rates.

CDS and the limits of body mass dependencies

Understanding the causes and consequences of extinctions, invasions and a range of other processes will depend acutely on resolving the scaling of consumer feeding rates: from a global-scale delineation according to MTE (Brown *et al.* 2004), through to the local-scale incorporating body mass ratios (Vucic-Pestic *et al.* 2010, 2011; Rall *et al.* 2012), towards finely resolved CDS.

The constituent parts of consumer feeding rates – capture rates and handling times – present several issues where the objective is to relate consumer feeding rates to stability in food webs. Handling times often exhibit a negative power law with increasing consumer mass (Vucic-Pestic *et al.* 2010; Pawar *et al.* 2012), but here we find an exponential decline similar to Aljetlawi *et al.* (2004). In part, this could result from the fixed experimental time and subsequent handling to digestion limitation transition with consumer size (see supplementary materials). Also, at small predator–prey body mass ratios aspects of interactions are not necessarily aligned with metabolic demand – for example, due to interference competition and intraguild predation (Barrios-O'Neill *et al.* 2014a).

Capture rates are widely observed – or assumed – to exhibit unimodal associations with consumer–resource body mass ratios (Persson *et al.* 1998; Vucic-Pestic *et al.* 2010; Pawar *et al.* 2012; Kalinkat *et al.* 2013). But we show here that the form of these unimodal associations can be context dependent (Fig. 2a–b), and disappear in certain contexts (Fig. 2c). In contrast, scaling exponents – as critical determinants of functional response shape (i.e. Type II or Type III) – often exhibit equivocal body mass dependency (Brose 2010; Vucic-Pestic *et al.* 2010), and we find evidence for Type II responses throughout our data (Fig. 2e). Because the link between functional response type and population stability can also be tenuous (Uszko *et al.* 2015), translating mass-based generalisations of consumer feeding to whole-community dynamics could be problematic. Despite this, CDS posits that defined changes in capture rate scaling – as opposed to ambiguous changes in functional response shape – remain a quantifiable modulator of consumer–resource coexistence.

Changes in capture rate scaling among contexts imply that CDS is inherently spatiotemporal, and suggest that scaling might even be inherently dynamic, but our non-sequential experiments cannot explicitly demonstrate this. Nevertheless, Fig. 5 qualitatively illustrates how local scaling might change if and when contexts change. Critically, the spatiotemporal consistency of dimensionality, structural complexity and other drivers will determine the degree to which size and temperature can act as standalone predictors of feeding rates. The corollary of this assertion is that CDS will be more prevalent where systems are characterised by changing consumer search strategies and associated heterogeneity, or where search strategies shift with ontogeny (Pawar *et al.* 2013). Even where heterogeneity typifies a system, CDS may not necessarily operate at a timescale relevant to population dynamics.

We propose that an underlying mechanism of CDS is the modification of consumer capture rates (Fig. 5), in the first instance via modification of the detection region (A_D) available

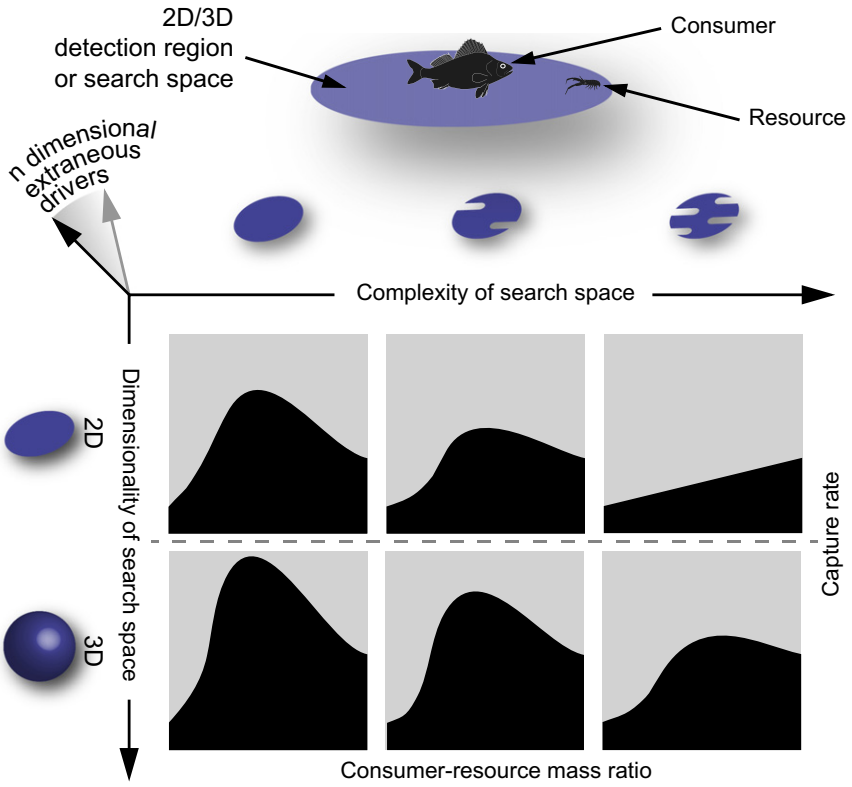

Figure 5 Context-Dependent Scaling of consumer feeding depends primarily on the modification of consumer capture rates which, in turn, depend on: (1) the relative velocity of consumer–resource pairs; (2) the dimensionality/size of detection regions (represented in blue) and (3) consumer–resource mass ratios. Consumer detection regions are reduced in 2D and also as complexity increases. Thus, capture rates can be lower in habitats of similar complexity if search spaces are 2D rather than 3D. Suboptimal capture rates (Fig. 1) result primarily from unsuccessful encounters, independently of detection region size. In contrast, optimal capture rates imply that a high proportion of encounters result in capture and, thus, that any reduction in detection region will disproportionately reduce encounters and capture. Together, these explain why unimodal scaling relationships can collapse in complex habitats (Fig. 2c).

to consumers and their resources (Fig. 5: blue regions) and, secondarily, through modification of the relative velocity (V_r) of consumers–resource pairs. A_D has already been mechanistically linked to dimensionality (Pawar *et al.* 2012) and structural complexity is known to modify both A_D and V_r (Manatunge *et al.* 2000), whereas other factors – such as dimensionality – may act primarily on A_D (Fig. 5).

A key empirical result of our study is the collapse of oft-observed unimodal distribution of capture rates (Figs 1 and 2a–c). In the extreme, resources are either too large or too small for consumers – meaning that resources are never consumed, regardless of encounter rate. At optimum ratios, however, a large proportion of encounters result in capture, implying that reductions in A_D will disproportionally reduce the capture rates of consumers foraging on optimally sized resources. Thus, hump-shaped scaling relationships can collapse in complex habitats where A_D is reduced (Fig. 2c).

Concluding remarks

Despite the long-recognised importance of body size in ecology (Elton 1927; Peters 1986; Woodward *et al.* 2005), it is only relatively recently that ecologists have begun to comprehensively resolve the body mass dependencies of consumer feeding rates (Vucic-Pestic *et al.* 2010; Pawar *et al.* 2015). We advance this area of inquiry by demonstrating the acute context dependency of capture rate scaling, and thus advocate the explicit consideration of CDS as a potentially important structuring mechanism in ecological networks.

ACKNOWLEDGEMENTS

We are grateful to Björn C. Rall for advice on fitting Ricker functions in R. The Ballinderry River Trust kindly loaned DBO salmonids for experimental trials and larger sticklebacks were obtained for experimental trials courtesy of Oxford Island Nature Reserve. Perch were obtained courtesy of Clune Fishery. We are grateful for the thoughtful and detailed comments of three reviewers that substantially improved the manuscript. We thank NSERC, Queen's University Belfast, the Natural Environment Research Council and the Department for Environment, Food and Rural Affairs (grant number NE/L003279/1, Marine Ecosystems Research Programme) for funding.

AUTHORSHIP

CDS concept and framework: DBO. Design and execution of experimental trials: DBO. Fitting functional responses and scaling models: DBO. Functional response surfaces: DBO and

RK. Dynamic population modelling: DBO, MCE and RK. First draft of the manuscript: DBO. Manuscript revisions: all authors.

REFERENCES

Aljetlawi, A.A., Sparrevik, E. & Leonardsson, K. (2004). Prey-predator size-dependent functional response: derivation and rescaling to the real world. *J. Anim. Ecol.*, 73, 239–252.

Barrios-O'Neill, D., Dick, J.T.A., Emmerson, M.C., Ricciardi, A., MacIsaac, H.J. & Alexander, M.E. *et al.* (2014a). Fortune favours the bold: a higher predator reduces the impact of a native but not an invasive intermediate predator. *J. Anim. Ecol.*, 83, 693–701.

Barrios-O'Neill, D., Dick, J.T.A., Ricciardi, A., MacIsaac, H.J. & Emmerson, M.C. (2014b). Deep impact: in situ functional responses reveal context-dependent interactions between vertically migrating invasive and native mesopredators and shared prey. *Freshw. Biol.*, 59, 2194–2203.

Barrios-O'Neill, D., Dick, J.T.A., Emmerson, M.C., Ricciardi, A. & MacIsaac, H.J. (2015). Predator-free space, functional responses and biological invasions. *Funct. Ecol.*, 29, 377–384.

Bolker, B.M. (2010). *bbmle: Tools for General Maximum Likelihood Estimation*. R Package.

Brose, U. (2010). Body-mass constraints on foraging behaviour determine population and food-web dynamics. *Funct. Ecol.*, 24, 28–34.

Brose, U., Williams, R.J. & Martinez, N.D. (2006). Allometric scaling enhances stability in complex food webs. *Ecol. Lett.*, 9, 1228–1236.

Brown, J.H., Gillooly, J.F., Allen, A.P., Savage, V.M. & West, G.B. (2004). Toward a metabolic theory of ecology. *Ecology*, 85, 1771–1789.

DeLong, J.P. (2014). The body-size dependence of mutual interference. *Biol. Lett.*, 10, 20140261.

Elton, C. (1927). *Animal Ecology*. University of Chicago Press, Chicago.

Englund, G. & Leonardsson, K. (2008). Scaling up the functional response for spatially heterogeneous systems. *Ecol. Lett.*, 11, 440–449.

Englund, G., Ohlund, G., Hein, C.L. & Diehl, S. (2011). Temperature dependence of the functional response. *Ecol. Lett.*, 14, 914–921.

Fryxell, J. (1995). Aggregation and migration by grazing ungulates in relation to resources and predators. In *Serengeti II: Dynamics, Management, and Conservation of an Ecosystem* (eds Sinclair, A.R.E. & Arcese, P.). University of Chicago Press, Chicago, pp. 257–273.

Holling, C.S. (1959). Some characteristics of simple types of predation and parasitism. *Can. Entomol.*, 91, 385–398.

Hutchinson, G.E. (1961). The paradox of the plankton. *Am. Nat.*, 95, 137–145.

Jeschke, J.M., Kopp, M. & Tollrian, R. (2004). Consumer-food systems: why type I functional responses are exclusive to filter feeders. *Biol. Rev.*, 79, 337–349.

Kalinkat, G., Schneider, F.D., Digel, C., Guill, C., Rall, B.C. & Brose, U. (2013). Body masses, functional responses and predator-prey stability. *Ecol. Lett.*, 16, 1126–1134.

Maino, J.L., Kearney, M.R., Nisbet, R.M. & Kooijman, S.A.L.M. (2014). Reconciling theories for metabolic scaling. *J. Anim. Ecol.*, 83, 20–29.

Manatunge, J., Asaeda, T. & Priyadarshana, T. (2000). The influence of structural complexity on fish–zooplankton interactions: a study using artificial submerged macrophytes. *Environ. Biol. Fishes*, 58, 425–438.

Murdoch, W.W. (1969). Switching in general predators: experiments on predator specificity and stability of prey populations. *Ecol. Monogr.*, 39, 335–354.

Noordhuis, R., Schie, J. & Jaarsma, N. (2009). Colonization patterns and impacts of the invasive amphipods *Chelicorophium curvispinum* and *Dikerogammarus villosus* in the IJsselmeer area, The Netherlands. *Biol. Invasions*, 11, 2067–2084.

Ohlund, G., Hedstrom, P., Norman, S., Hein, C.L. & Englund, G. (2014). Temperature dependence of predation depends on the relative performance of predators and prey. *Proc. R. Soc. London. Ser. B Biol. Sci.*, 282, 20142254.

Osenberg, C.W. & Mittelbach, G.G. (1989). Effets of body size on the predator-prey interaction between pumpkinseed sunfish and gastropods. *Ecol. Monogr.*, 59, 405–432.

Paterson, R.A., Pritchard, D.W., Dick, J.T.A., Alexander, M.E., Hatcher, M.J. & Dunn, A.M. (2013). Predator cue studies reveal strong trait-mediated effects in communities despite variation in experimental designs. *Anim. Behav.*, 86, 1301–1313.

Pawar, S., Dell, A.I. & Savage, V.M. (2012). Dimensionality of consumer search space drives trophic interaction strengths. *Nature*, 486, 485–489.

Pawar, S., Dell, A.I. & Savage, V.M. (2013). Pawar *et al.* reply. *Nature*, 493, E2–E3.

Pawar, S., Dell, A.I. & Savage, V.M. (2015). From metabolic constraints on individuals to the dynamics of ecosystems. In *Aquatic Functional Biodiversity: An Ecological and Evolutionary Perspective* (eds Belgrano, A., Woodward, G. & Jacob, U.). Academic Press, London, pp. 3–36.

Persson, L., Leonardsson, K., de Roos, A.M., Gyllenberg, M. & Christensen, B. (1998). Ontogenetic scaling of foraging rates and the dynamics of a size-structured consumer-resource model. *Theor. Popul. Biol.*, 54, 270–293.

Peters, R. (1986). *The Ecological Implications of Body Size (Vol 2)*. Cambridge University Press, Cambridge.

Rall, B.C., Kalinkat, G., Ott, D., Vucic-Pestic, O. & Brose, U. (2011). Taxonomic versus allometric constraints on non-linear interaction strengths. *Oikos*, 120, 483–492.

Rall, B.C., Brose, U., Hartvig, M., Kalinkat, G., Schwarzmüller, F. & Vucic-Pestic, O. *et al.* (2012). Universal temperature and body-mass scaling of feeding rates. *Philos. Trans. R. Soc. Lond. B Biol. Sci.*, 367, 2923–2934.

Real, L.A. (1977). The kinetics of functional response. *Am. Nat.*, 111, 289–300.

van Riel, M.C., Van Der Velde, G., Rajagopal, S., Marguillier, S., Dehairs, F. & de Vaate, A.B. (2006). Trophic relationships in the Rhine food web during invasion and after establishment of the Ponto-Caspian invader Dikerogammarus villosus. *Hydrobiologia*, 565, 39–58.

Rogers, D. (1972). Random search and insect population models. *J. Anim. Ecol.*, 41, 369–383.

Rosenzweig, M.L. & Macarthur, R. (1963). Graphical representations and stability conditions of predator-prey interactions. *Am. Nat.*, 97, 209–223.

Schneider, F.D., Scheu, S. & Brose, U. (2012). Body mass constraints on feeding rates determine the consequences of predator loss. *Ecol. Lett.*, 15, 436–443.

Toscano, B.J. & Griffen, B.D. (2014). Trait-mediated functional responses: predator behavioural type mediates prey consumption. *J. Anim. Ecol.*, 83, 1469–1477.

Uszko, W., Diehl, S., Pitsch, N., Lengfellner, K. & Müller, T. (2015). When is a type III functional response stabilizing? Theory and practice of predicting plankton dynamics under enrichment. *Ecology*, 96, 3243–3256.

Van den Brink, F.W.B., Van der Velde, G. & Bij de Vaate, A. (1993). Ecological aspects, explosive range extension and impact of a mass invader, *Corophium curvispinum* Sars, 1895 (Crustacea: Amphipoda), in the Lower Rhine (The Netherlands). *Oecologia*, 93, 224–232.

Vonesh, J.R. & Bolker, B.M. (2005). Compensatory larval responses shift trade-offs associated with predator-induced hatching plasticity. *Ecology*, 86, 1580–1591.

Vucic-Pestic, O., Rall, B.C., Kalinkat, G. & Brose, U. (2010). Allometric functional response model: body masses constrain interaction strengths. *J. Anim. Ecol.*, 79, 249–256.

Vucic-Pestic, O., Ehnes, R.B., Rall, B.C. & Brose, U. (2011). Warming up the system: higher predator feeding rates but lower energetic efficiencies. *Glob. Chang. Biol.*, 17, 1301–1310.

Wahlström, E., Persson, L. & Diehl, S. (2000). Size-dependent foraging efficiency, cannibalism and zooplankton community structure. *Oecologia*, 123, 138–148.

Williams, R.J. & Martinez, N.D. (2004). Stabilization of chaotic and non-permanent food-web dynamics. *Eur. Phys. J. B Condens. Matter Complex Syst.*, 38, 297–303.

Woodward, G., Ebenman, B., Emmerson, M., Montoya, J.M., Olesen, J.M. & Valido, A. *et al.* (2005). Body size in ecological networks. *Trends Ecol. Evol.*, 20, 402–409.

SUPPORTING INFORMATION

Additional Supporting Information may be downloaded via the online version of this article at Wiley Online Library (www.ecologyletters.com).

Editor, Greg Grether
Manuscript received 4 February 2016
First decision made 23 February 2016
Manuscript accepted 11 March 2016